Transactions of the KSNVE, 23(3) : 240~248, 2013
http://dx.doi.org/10.5050/KSNVE.2013.23.3.240

한국소음진동공학회논문집 제 23 권 제 3 호, pp. 240~248, 2013
ISSN 1598-2785(Print), ISSN 2287-5476(Online)

Study on the Dynamic Characteristics of a Manual Transmission Using Linear Models

선형모델을 이용한 수동변속기의 동적 특성 연구

Jong-Yun Yoon* and Iljae Lee†
윤 종 윤 · 이 일 재

(Received December 4, 2012 ; Revised February 18, 2013 ; Accepted February 18, 2013)

Key Words : Gear(기어), Linear Model(선형모델), Dual-mass Flywheel(이중질량 플라이휠)

ABSTRACT

Torsional vibrations, such as the gear rattle of the manual transmission in vehicle systems, are correlated with the firing stroke from the engine. These vibro-impacts can be examined based upon linear time-invariant analysis. In order to understand the gear dynamics, a specific manual transmission with a front-engine front-wheel drive configuration is investigated. A method to reduce the degrees of freedom is suggested based upon the eigensolutions and frequency response functions, which will lead to the development of an efficient matrix size. The dynamic characteristics of single- and dual-mass flywheels are then compared. The effect of the dual-mass flywheel is investigated based upon the mobility analysis, which will lead to understanding of the concepts for avoiding vibro-impacts. A linear time-invariant system model is examined by employing the effective clutch stiffness from a two-stage clutch damper. Thus, the relationship between the dynamic characteristics and the clutch damper can be predicted by assuming a combination of different stage stiffness levels.

요 약

자동차 수동변속기 내 래틀과 같은 회전체 진동은 엔진 연소폭발 주기와 연동하여 발생한다. 이러한 충격형 진동 특성은 선형 시간 불변 분석법을 적용하여 살펴볼 수 있다. 기어의 동적 특성을 이해하기 위해, 특정 형태의 앞 바퀴 굴림 방식 수동 변속기에 대한 연구를 수행하였다. 첫째, 동특성 고유값과 주파수 응답함수를 기반으로 자유도를 줄이는 방법을 제시하였는데, 이는 행렬의 크기를 줄이는 효과적인 역할을 한다. 둘째, 단일 질량 플라이휠과 이중 질량 플라이휠의 동적 특성을 비교하였다. 모빌리티 분석을 기반으로 한 이중 질량 플라이휠의 효과를 검토하였는데, 이로부터 진동에 의해 가진되는 충격을 회피하기 위한 기본 개념을 이해 할 수 있다. 마지막으로, 두 단계 클러치 댐퍼로부터 유효 강성 값을 도출하여 선형 불변형 시스템 모델을 연구하였다. 두 단계의 서로 다른 클러치 강성조합을 이용하여 클러치 댐퍼의 동적특성에 대한 관계를 예측할 수 있다.

† Corresponding Author ; Member, Department of Mechanical Engineering, Chonbuk National University
E-mail : leeij@jbnu.ac.kr
Tel : +82-63-270-2319, Fax : +82-63-270-2315
* STX Heavy Industry Co.

‡ Recommended by Editor Don Chool Lee

Nomenclature

I : Inertia
R : Gear radius
k : Spring stiffness

Subscripts
c : Clutch
d : Differential
f : Flywheel
g : Gear mesh
h : Clutch hub
i : Input shaft
ir : Reverse gear on input shaft
$i\#$: #th gear on input shaft
jl : Left cv joint
jr : Right cv joint
o : Output shaft
od : Final gear on output shaft
or : Reverse gear on output shaft
$o\#$: #th gear on output shaft
ri : Idler
t : Tie and rotor
v : Vehicle
$v1$: Left drive shaft
$v2$: Right drive shaft

1. Introduction

In many torsional systems, such as vehicle transmissions and heavy-duty engines, vibro-impacts are induced by gear backlash, multi-staged clutch characteristics, and other clearance type nonlinearities[1~12]. Such vibro-impacts result in excessive noise and vibration and degrade the vehicle sound quality. Given the high costs associated with experimental methods[1~6], simulation methods are preferred for diagnosing problems and designing transmissions[7~11]. The driveline system is typically modeled as a lumped-parameter torsional system. To describe the lumped system of a real transmission, linear system analysis with a focus on eigensolutions is carried out as a first step[13]. Rattle phenomena are then investigated based on simulation models with two or more nonlinearities[7~11,14]. Thus, understanding proper linear models, in addition to the nonlinearities, is essential to driveline research.

In this study, a real physical manual transmission was examined with respect to the torsional vibration based on the modal analysis and frequency response functions with the unit torque input. Figure 1 shows a schematic description of a torsional model with 14 degrees of freedom(DOF). The gears indicated with cross lines illustrate the speed gear, which is always unloaded and rotating unless it is not engaged through the synchronizer by the driver's gear-shifting mechanism. Each component is described by the lumped inertia or stiffness: these include the flywheel, clutch hub, input shaft, gear pairs, axles, and tire-vehicle. The synchronizer assembly and fixed gears are assumed to be lumped into the input and output shafts. The scope of this study was limited to the engine torque profile for a front-engine front-wheel type driveline when the third gear is engaged and fifth gear is unloaded.

The chief objectives of this research are as follows: (1) develop a linear torsional model and examine system responses in the frequency domain; (2)

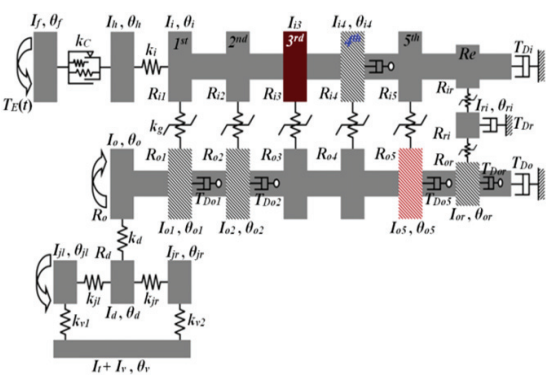

Fig. 1 Schematic of the driveline system: lumped torsional model with 14-DOF

reduce the DOF of the original torsional system model and compare the dynamic characteristics of the original and reduced systems(To reduce the number of DOF by preserving the nature of the original system, the dynamic characteristics based upon the eigensolutions and frequency responses of the reduced and original systems should show the same results); (3) investigate the effect of a dual-mass flywheel(DMF) by comparing it to a single-mass flywheel(SMF) based on dynamic characteristics and frequency response functions; and (4) examine the effective clutch stiffness from a two-staged clutch damper by using the linear time-invariant system model.

2. Linear Models

In this study, physical models of a transmission (with third gear engaged and fifth gear unloaded) with 14 and 6 DOF were analyzed under the wide-open-throttle(WOT) condition. In order to examine the dynamic characteristics of the linear time-invariant(LTI) system, the following assumptions were made: (1) the system is a torsional semi-definite system; (2) nonlinearities such as clutch hysteresis and gear backlash can be ignored; (3) gears are always in contact on the driving side, resulting in a rattle-free system[11,15]; (4) this LTI system model has a single clutch stiffness value.

2.1 14-DOF Model

The schematic of the 14-DOF system is constructed by including other subsystems, such as the flywheel, drive shaft, and vehicle, as shown in Fig. 1. This 14-DOF model shows that the first, second, fifth, and reverse input gears are "welded" to the input shaft. Likewise, the third and fourth gears are "welded" to the output shaft. The basic equations for the 14-DOF model were derived based upon the schematic shown in Fig. 1. In order to examine the eigensolutions, the torque excitation vector and damping matrix were ignored. $\underline{\boldsymbol{\theta}}(\mathbf{t})$ is the absolute torsional displacement, $\underline{\underline{\mathbf{M}}}$ is the inertia matrix, and $\underline{\underline{\mathbf{K}}}$ is the stiffness matrix:

$$\underline{\underline{\mathbf{M}}}\,\ddot{\underline{\boldsymbol{\theta}}}(\mathbf{t})+\underline{\underline{\mathbf{K}}}\,\underline{\boldsymbol{\theta}}(\mathbf{t})=\underline{\mathbf{0}} \tag{1}$$

$$\underline{\boldsymbol{\theta}}=\left[\theta_f\ \ \theta_h\ \ \theta_i\ \ \theta_o\ \ \theta_{ol}\ \ \theta_{o2}\ \ \theta_{o5}\ \ \theta_{ri}\ \ \theta_{or}\ \ \theta_{i4}\ \ \theta_d\ \ \theta_{jl}\ \ \theta_{jr}\ \ \theta_v\right]^{\mathrm{T}} \tag{2}$$

$$\underline{\underline{\mathbf{M}}}=diag\left[I_f, I_h, (I_i+I_{i3}), I_o, I_{ol}, I_{o2}, I_{o5}, I_{ri}, I_{or}, I_{i4}, I_d, I_{jl}, I_{jr}, (I_v+I_t)\right] \tag{3}$$

$$\underline{\underline{\mathbf{K}}}=\begin{bmatrix} & k(i,j) & \end{bmatrix} \tag{4}$$

$$k_{1,1}=k_C,\quad k_{2,2}=k_C+k_i \tag{5a,b}$$

$$k_{3,3}=k_i+k_g\left(R_{i1}{}^2+R_{i2}{}^2+R_{i3}{}^2+R_{i5}{}^2+R_{ir}{}^2\right) \tag{6}$$

$$k_{4,4}=k_g\left(R_{o3}{}^2+R_{o4}{}^2\right)+k_dR_{od}{}^2 \tag{7}$$

$$k_{5,5}=k_gR_{o1}{}^2,\quad k_{6,6}=k_gR_{o2}{}^2 \tag{8a,b}$$

$$k_{7,7}=k_gR_{o5}{}^2,\quad k_{8,8}=2k_gR_{ri}{}^2 \tag{9a,b}$$

$$k_{9,9}=k_gR_{or}{}^2,\quad k_{10,10}=k_gR_{i4}{}^2 \tag{10a,b}$$

$$k_{11,11}=k_dR_d{}^2+k_{jl}+k_{jr},\quad k_{12,12}=k_{jl}+k_{v1} \tag{11a,b}$$

$$k_{13,13}=k_{jr}+k_{v2},\quad k_{14,14}=k_{v1}+k_{v2} \tag{12a,b}$$

$$k_{1,2}=k_{2,1}=-k_C,\quad k_{2,3}=k_{3,2}=-k_i \tag{13a,b}$$

$$k_{3,4}=k_{4,3}=k_gR_{i3}R_{o3},\quad k_{3,5}=k_{5,3}=k_gR_{i1}R_{o1} \tag{14a,b}$$

$$k_{3,6}=k_{6,3}=k_gR_{i2}R_{o2},\quad k_{3,7}=k_{7,3}=k_gR_{i5}R_{o5} \tag{15a,b}$$

$$k_{3,8}=k_{8,3}=k_gR_{ir}R_{ri},\quad k_{4,10}=k_{10,4}=k_gR_{i4}R_{o4} \tag{16a,b}$$

$$k_{4,11}=k_{11,4}=k_dR_{od}R_d,\quad k_{8,9}=k_{9,8}=k_gR_{ri}R_{or} \tag{17a,b}$$

$$k_{11,12}=k_{12,11}=-k_{jl},\quad k_{11,13}=k_{13,11}=-k_{jr} \tag{18a,b}$$

$$k_{12,14}=k_{14,12}=-k_{v1},\quad k_{13,14}=k_{14,13}=-k_{v2} \tag{19a,b}$$

Here, the unit of the gear mesh stiffness k_g is N·m^{-1} and other torsional stiffness terms(e.g., k_C, k_i etc.) have the unit of N·m·rad^{-1} as described in Table 1.

2.2 6-DOF Model

The 14-DOF model developed in the previous section may reflect the dynamic behavior of the system shown in Fig. 1 in detail. However, such large dimensions may be troublesome for non-linear analysis[4,9,11]. Thus, the system can be reduced into a 6-DOF model, as shown in Fig. 2. In the resulting system, all inertia and stiffness values of gear pairs, except for the other properties shown in Fig. 2, are replaced by the gear ratio-squared $(R_1/R_2)^2$ values, where R is the gear radius[9,16,17]. The reduced system is expressed by the same formulation as Eq. (1):

$$\underline{\boldsymbol{\theta}} = \left[\theta_f \quad \theta_h \quad \theta_i \quad \theta_{ou} \quad \theta_{OG} \quad \theta_v\right]^{\mathrm{T}} \tag{20}$$

$$\underline{\underline{\mathbf{M}}} = diag\left[I_f, I_h, I_{ie}, I_{ou}, I_{OG}, I_{VE2}\right] \tag{21}$$

$$\underline{\underline{\mathbf{K}}} = \begin{bmatrix} k_C & -k_C & 0 & 0 & 0 & 0 \\ -k_C & k_C+k_i & -k_i & 0 & 0 & 0 \\ 0 & -k_i & k_i+k_g\left(R_{iu}^2+R_{ie}^2\right) & k_gR_{iu}R_{ou} & k_gR_{ie}R_{oe} & 0 \\ 0 & 0 & k_gR_{iu}R_{ou} & k_gR_{ou}^2 & 0 & 0 \\ 0 & 0 & k_gR_{ie}R_{oe} & 0 & k_gR_{oe}^2+k_{VE2} & -k_{VE2} \\ 0 & 0 & 0 & 0 & -k_{VE2} & k_{VE2} \end{bmatrix} \tag{22}$$

$$I_{ie} = I_i + I_{i3} + \left(R_{i1}/R_{o1}\right)^2 I_{o1} + \left(R_{i2}/R_{o2}\right)^2 I_{o2} + \left(R_{ir}/R_{ri}\right)^2 \left(I_{ri} + \left(R_{ri}/R_{or}\right)^2 I_{or}\right) \tag{23}$$

$$I_{oe} = I_o + \left(R_{o4}/R_{i4}\right)^2 I_{i4} \tag{24}$$

$$I_{de} = I_d + \frac{I_{jl}+I_{jr}}{2} \tag{25}$$

$$I_{ve} = I_t + I_v + \frac{I_{jl}+I_{jr}}{2} \tag{26}$$

$$I_{OG} = I_{oe} + \left(R_{od}/R_d\right)^2 I_{de}, \quad I_{VE2} = \left(R_{od}/R_d\right)^2 I_{ve} \tag{27a,b}$$

$$k_{eq} = \frac{k_{jl}k_{v1}}{k_{jl}+k_{v1}} + \frac{k_{jr}k_{v2}}{k_{jr}+k_{v2}}, \quad k_{VE2} = \left(R_{od}/R_d\right)^2 k_{eq} \tag{28a,b}$$

Refer to the nomenclature and Fig. 2 for the symbols used in Eqs. (20)~(28). The models given by Eqs. (1)~(4) and (20)~(22) are used to obtain the eigensolution of the system while ignoring the damping and input. However, in order to calculate the frequency response functions, the damping and input or excitation need to be considered. Thus, the 6-DOF model should be assessed by the frequency response functions as given by Eq. (29).

$$\underline{\underline{\mathbf{M}}}\,\ddot{\underline{\boldsymbol{\theta}}}(\mathbf{t}) + \underline{\underline{\mathbf{C}}}\,\dot{\underline{\boldsymbol{\theta}}}(\mathbf{t}) + \underline{\underline{\mathbf{K}}}\,\underline{\boldsymbol{\theta}}(\mathbf{t}) = \underline{\mathbf{T}}(\mathbf{t}) \tag{29}$$

Considering the damped and forced responses of torsional system under sinusoidal excitation, $\underline{\underline{\mathbf{C}}}$ is the viscous damping matrix, and $\underline{\mathbf{T}}(\mathbf{t})$ is the torque excitation vector. The modal damping ratios are assumed to be equal to 5 % for all modes. We then obtain the viscous damping matrix using the normal modal matrix and damping ratios[11,16]. The harmonic torque at the engine is applied by assuming the unit value as given by Eq. (30).

$$\underline{\mathbf{T}}(\mathbf{t}) = \left[I \quad 0 \quad 0 \quad 0 \quad 0 \quad 0\right]^{\mathrm{T}} e^{i\omega_o t} \tag{30}$$

Now, the torsional mobility $Y_{\alpha j}(\omega_o)$ and motion

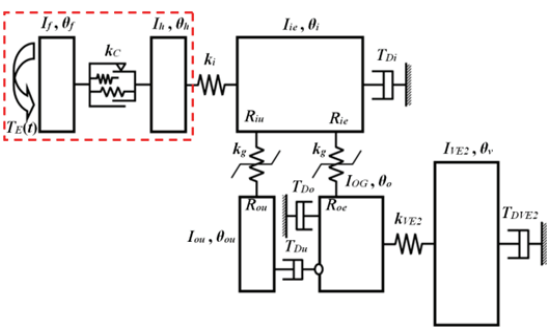

Fig. 2 Reduced order system model when the third gear is engaged and fifth gear is unloaded: 6-DOF system model with SMF

transmissibility $TR_{\alpha j}(\omega_o)$ are defined by Eqs. (31) and (32), where subscripts α and j are the excitation and input locations, respectively, at the relevant subsystem, and ω_o is the excitation frequency.

$$Y_{\alpha j}(\omega_o)=\frac{\dot{\theta}_\alpha}{T_j}(\omega_o) \tag{31}$$

$$TR_{\alpha j}(\omega_o)=\frac{\dot{\theta}_\alpha}{\dot{\theta}_j}(\omega_o) \tag{32}$$

3. Simulation Results

3.1 Operating Conditions

In order to identify the operating conditions with respect to gear rattle phenomena, experimental results were analyzed. Fig. 3 shows a representative example of system responses measured from the engine and transmission. The measured data shown in Fig. 3 illustrate the acceleration $\tilde{\Psi}_M$ (in the unit of rad·s^{-2}) as a function of the speed. Given the limited experimental data, rattle phenomena were assumed to occur when the gearbox acceleration exceeded the engine acceleration. This study focused on the vehicle driving conditions under WOT with 1800 RPM. An LTI system model was developed based upon the given measured data and system parameters. Tables 1~3 list the employed properties given by a transmission manufacturer and their designations.

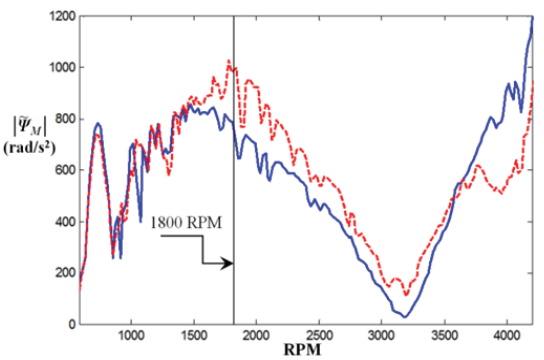

Fig. 3 Measured accelerations on the powertrain under the WOT condition : ——, on engine ; - - - -, on transmission

3.2 Comparisons between 14– and 6–DOF Models

Equations (1)~(28) were used to determine the natural frequencies and mode shapes of the 14- and 6-DOF system models. Table 4 and Fig. 4 present the first three natural frequencies and mode shapes for both models. In Fig. 4, the mode shape at 60 Hz can be interpreted as being controlled by the clutch

Table 1 Stiffness employed in simulations

Stiffness	Values(N·m·rad^{-1})	Stiffness	Values(N·m^{-1})
k_i	10,000	k_g	2.7×10^{8}
k_{jl}, k_{jr}	10,000	k_d	2.7×10^{8}
k_{v1}, k_{v2}	10,000		
k_C	1,838		

Table 2 Inertia employed in simulations

Inertial	Values(kg·m^2)	Inertial	Values(kg·m^2)
I_f	1.38×10^{-1}	I_{o5}	5.23×10^{-4}
I_h	5.76×10^{-3}	I_{ri}	4.35×10^{-4}
I_i	3.10×10^{-3}	I_{or}	1.33×10^{-3}
I_o	5.33×10^{-3}	I_d	2.15×10^{-2}
I_{i3}	5.80×10^{-4}	I_{jl}	3.91×10^{-3}
I_{i4}	8.73×10^{-4}	I_{jr}	4.35×10^{-3}
I_{o1}	2.60×10^{-3}	I_t	2.80×10^{-1}
I_{o2}	1.39×10^{-3}	I_v	48.94

Table 3 Gear radii employed in simulations

Radius	Values(10^{-3} m)	Radius	Values(10^{-3} m)
R_{i1}	18.30	R_{o2}	51.99
R_{i2}	29.51	R_{o3}	46.01
R_{i3}	35.50	R_{o4}	39.55
R_{i4}	41.95	R_{o5}	35.58
R_{i5}	45.92	R_{or}	54.95
R_{ir}	16.36	R_{od}	26.63
R_{ri}	40.14	R_d	103.37
R_{o1}	63.20		

or axle stiffness. These characteristics were also seen in the simulation using the 6-DOF model. Fig. 5 compares the mobility spectra of the 6- and 14-DOF systems in terms of the magnitude of mobility vs. frequency. $|Y_{ff}|$, $|Y_{hf}|$, and $|Y_{if}|$ are defined as the mobilities of the flywheel, clutch hub, and input shaft, respectively. As shown in Fig. 5, the resonances of $|Y_{ff}|$ and $|Y_{hf}|$ were seen at 7 and 60 Hz. Resonances of $|Y_{if}|$ were observed at 7, 60 and 273 Hz. The mobilities of the 6-DOF model matched well with those of the 14-DOF model, as shown in Fig. 5. Therefore, the 6-DOF model was used for further system analysis.

Table 4 Comparison of natural frequencies for the 6- and 14-DOF systems

Frequency(Hz)	6-DOF	14-DOF
f_1	7.6	7.6
f_2	60.6	60.8
f_3	273	272

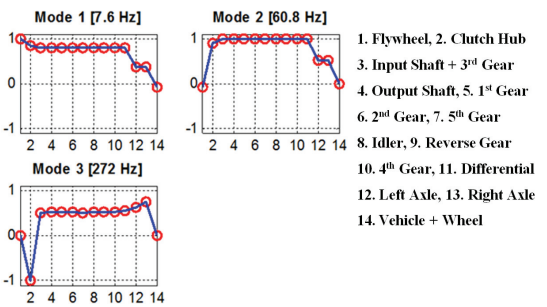

(a) 14-DOF system

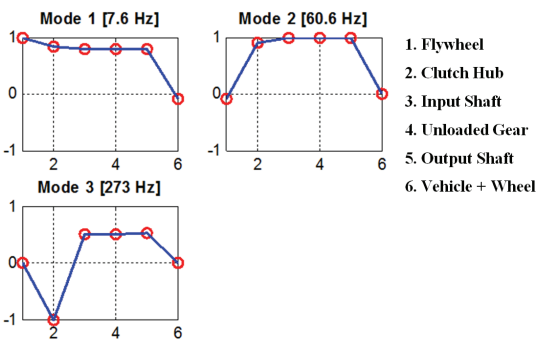

(b) 6-DOF system

Fig. 4 Comparison of mode shapes

3.3 Effect of Dual-mass Flywheel

The dual-mass flywheel is often used to solve rattle problems since it can decouple the engine's rotational irregularities. A DMF generally consists of two inertial parts—a primary and secondary flywheel—along with a single- or multi-staged torsioinal damper and some hysteresis that is installed between the primary and secondary masses[7,18].

Fig. 6 shows a schematic of a DMF based upon subsystems marked with the dotted line of the 6-DOF model from Fig. 2. The reduced model embedded with a DMF, as illustrated in Fig. 6, was then constructed with 7 DOF. The following properties were employed: DMF stiffness k_f = 562.1 N·m·rad^{-1}; clutch stiffness k_C = 10,000 N·m·rad^{-1}; inertia of first mass flywheel $I_{fa} = 0.7 \times I_f$; and inertia of second mass flywheel $I_{fb} = 0.7 \times I_f$.

When an engine has a DMF instead of an SMF, the clutch generally does not have a multi-staged clutch damper since the DMF has the key role of absorbing the fluctuation from the engine with the multi-staged torsional damper. Fig. 7 compares two different mode shapes for the SMF and DMF. With the DMF, a new mode at 22.9 Hz was generated, and 60.6 Hz shifted to 124 Hz.

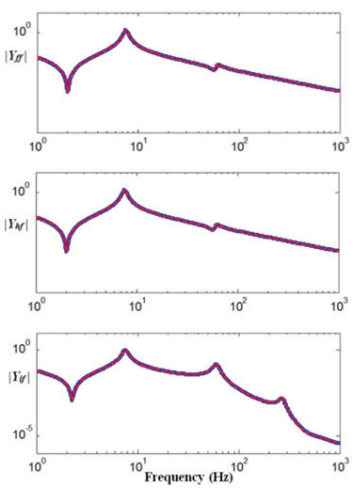

Fig. 5 Comparison of mobility spectra: ——, 14-DOF system; - - - -, 6-DOF system

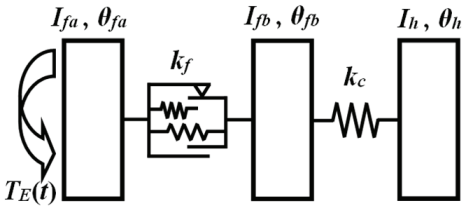

Fig. 6 Schematic of DMF

Table 5 Comparison of natural frequencies between SMF and DMF

Mode Descriptions	Natural frequencies(Hz)	
	SMF	DMF
Driveline surging mode	7.6	7.1
Flywheel mode	—	22.9
Clutch spring mode	60.6	124

Table 5 compares the natural frequencies and their mode descriptions of the SMF and DMF systems. Figure 8 compares the transmissibilities of an SMF and DMF; the subscripts i and f indicate the input shaft and flywheel, respectively. In general, the gear rattle can be measured at a reference point (i.e., flywheel) and dynamic response point (i.e., input shaft). Figure 8 shows that the DMF reduced the transmissibility level more effectively than the SMF. In this case, the resonance of the SMF was divided into two frequency ranges when DMF was used: 23 and 124 Hz. This is shown in Fig. 7 and Table 5.

3.4 Effect of Two-stage Clutch

As discussed in the previous sections, the system characteristics of the 14-DOF and 6-DOF models were examined. The results are based on the assumption that the clutch damper is linear with only one stage and that no hysteresis is present. However, real clutch dampers may exhibit multi-stage hysteresis, preload effects, and stoppers. Therefore, only a limited range of natural frequencies may be simulated by a linear model. Figure 9 shows the static torque (T_C) vs. relative torsional displacement across the clutch (δ_1)

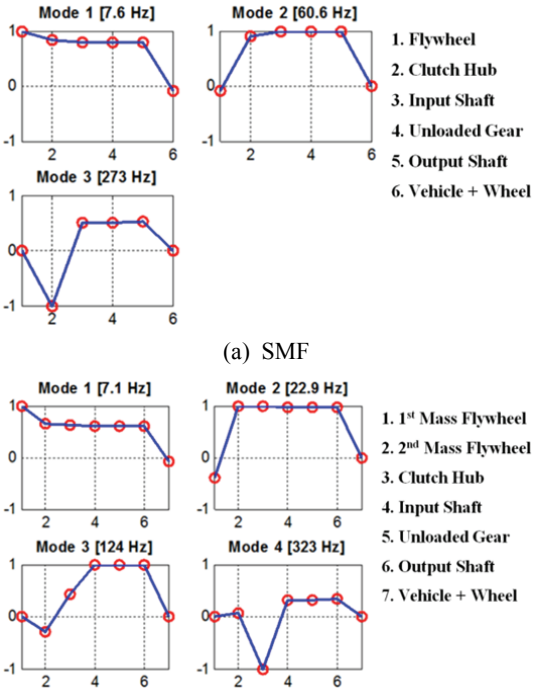

Fig. 7 Mode shapes of the reduced order system

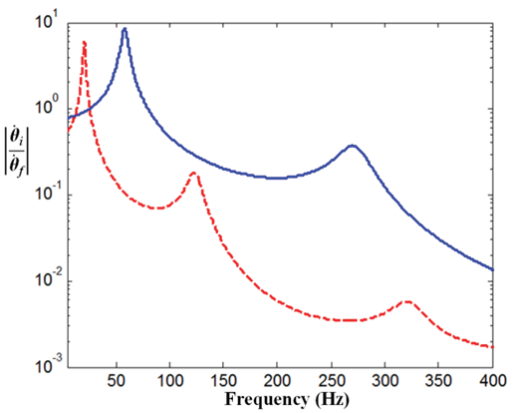

Fig. 8 Motion transmissibility of the reduced order system: ——, SMF ; - - - -, DMF

curve for two different clutch stiffness areas. The clutch illustrated in Fig. 9 has four stages with symmetric transition angles. If this clutch experiences the given mean torque range as marked by the dotted lines in Fig. 9, different eigensolutions may result depending on the effective clutch stiffness. For example, the dynamic torque range

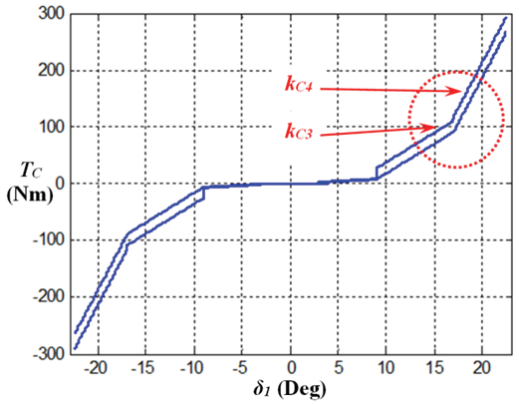

Fig. 9 Characteristics of multi-stage clutch damper with expected dynamic torque area

Table 6 Natural frequencies with a multi-stage clutch

Simulations(Hz)					Measurement (Hz)
k_{c3}=595.8 N·m·rad^{-1}	k_{c4}=1838 N·m·rad^{-1}	k_{c3}:k_{c4}			
		30:70	20:80	10:90	
40.6	60.6	55.6	57.3	59.0	60.0

marked in Fig. 9 may cross the stiffness transitions. Thus, the driveline system may show different characteristics corresponding to effective clutch stiffness levels. With this static response, several assumptions are possible. For example, Table 6 shows the three possible clutch damper responses. Two stages of the clutch dampers—third and fourth—were assumed to operate under the pulsating torque condition. Therefore, the third stage can operate for x % of the time, and the fourth stage operates for $(100-x)$ %. With this assumption, combinations can be allotted to each clutch damper as shown in Table 6. The simulation result of 59.0 Hz under the assumption of kc_3:kc_4=10:90 was close to the measured frequency of 60 Hz. Thus, a multi-stage clutch seems to spend more time in the fourth stage.

4. Conclusion

This study investigated the torsional vibration in a vehicle system with manual transmission using a specific clutch. In order to examine the dynamic characteristics based upon the linear time-invariant system model, a real physical driveline was modeled. The system was then reduced into 6-DOF from 14-DOF. The conclusions are summarized as follows. First, a method to reduce the DOF was introduced based upon the eigensolutions and frequency response functions. This contributed to reducing the calculation time for highly nonlinear system models with clearance-type nonlinearities; this will be the subject of further study. Second, the effect of DMF was investigated by comparing the mobilities of SMF and DMF torsional systems. This led to an understanding of the concepts for avoiding vibro-impacts. Finally, a linear study was conducted by considering the effective clutch stiffness from a multi-stage clutch damper. Thus, the dynamic conditions of a clutch spring can be predicted by assuming combinations of different stage stiffnesses.

References

(1) Couderc, P., Callenaere, J., Hagopian, J. D. and Ferraris, G., 1998, Vehicle Driveline Dynamic Behavior: Experimentation and Simulation, Journal of Sound and Vibration, Vol. 218, No. 1, pp. 133~157.

(2) Chikatani, Y. and Suehiro, A., 1991, Reduction of Idling Rattle Noise in Trucks, SAE 911044, pp. 49~56.

(3) Howell, T. P., Powell, N. N. and Etheridge, P., 2002, The Application of Correlated Modeling Techniques to Investigate Gear Rattle Noise in a Harley-Davidson Motorcycle, Inter-Noise 2002 Proceedings, pp. 2469~2477.

(4) Shimizu, T., 1993, Mechanism of the Idle Gear Rattle Synchronized with Engine Rotation, SAE 932003 pp. 7~13.

(5) Barthod, M., Hayne, B., Tebec, J. L. and Pin, J. C., 2007, Experimental Study of Gear Rattle Excited by a Multi-harmonic Excitation, Applied Acoustics 68, pp. 1003~1025.

(6) Rocca, E. and Russo, R., 2011, Theoretical and Experimental Investigation Into the Influence of the

Periodic Backlash Fluctuations on the Gear Rattle, Journal of Sound and Vibration, Vol. 330, pp. 4738~4752.

(7) Laschet, A., 1994, Computer Simulation of Vibration in Vehicle Powertrains Considering Nonlinear Effects in Clutches and Manual Transmissions, SAE 941011, pp. 1~8.

(9) Padmanabhan, C., Rook, T. E. and Singh, R., 1995, Modeling of Automotive Gear Rattle Phenomenon: State of the Art, SAE 951316, pp. 669~680.

(10) Padmanabhan, C. and Singh, R., 1993, Influence of Clutch Design on the Reduction and Perception of Automotive Transmission Rattle Noise, Noise-Con 93 Proceedings, pp. 607~612.

(11) Singh, R., Xie, H. and Comparin, R. J., 1989, Analysis of Automotive Neutral Gear Rattle, Journal of Sound and Vibration, Vol. 131, pp. 177~196.

(12) Hong, D. P., Chung, T. J. and Tae, S. H., 1994, A Study for the Torsional Characteristics of Clutch and Automotive Neutral Gear Rattle, Proceedings of the KSNVE Annual Autumn Conference, pp. 100~105.

(13) Ahn, M. J., Cho, S. M., Yoon, J. Y., Kim, J. S. and Lyu, S. K., 2007, Linear Analysis of Geared System with a Manual Transmission, Journal of the Korean Society of Safety, Vol. 22, No. 5, pp. 1~6.

(14) Ahn, M. J., Lyu, S. K., Yoon, J. Y., Qi, Z. and Ahn, I. H., 2010, A Study of the Linear Analysis for Nonlinear Torsional System, Journal of the Korean Society of Manufacturing Process Engineers, Vol. 9, No. 2, pp. 12~19.

(15) Kim, T. C. and Singh, R., 2001, Dynamic Interactions between Loaded and Unloaded Gears, SAE Transactions, Vol. 110, Section 6, pp. 1934~1943.

(16) Trochon, E. P., 1997, Analytical Formulation of Automotive Drivetrain Rattle Problems, MS Thesis, The Ohio State University.

(17) Hartog, J. P., 1985, Mechanical Vibrations, Dover, pp. 351~353.

(18) Gaillard, C. L. and Singh, R., 2000, Dynamic Analysis of Automotive Clutch Dampers, Applied Acoustics, Vol. 60, pp. 399~424.

Jong-Yun Yoon received his PhD from the Department of Mechanical Engineering at Ohio State University. He is currently working at STX Heavy Industries Co. as a senior engineer. His research interests are in automotive NVH, including nonlinear torsional vibration.

Iljae Lee received his PhD from the Department of Mechanical Engineering at Ohio State University. He is currently an assistant professor at Chonbuk National University. His research interests are in automotive NVH.